severely immunodeficient NOG mice enabled mouse liver to be stably replaced with mature and functional human liver tissue in the absence of ongoing drug treatment.

2. Materials and methods

2.1. Transgenic mice, human liver cell transplantation and drug biotransformation analysis

The herpes simplex virus type 1 thymidine kinase (*UL23* or HSVtk) gene expression unit was constructed as in Fig. S1A. A vector-free 4.4-kb HSVtk expression fragment was microinjected into fertilized NOD/Shi strain mouse eggs using standard methods. For further information about the creation and breeding of the TK-NOG strain, human liver cell transplantation, and the drug biotransformation studies, see supplementary materials and methods. This study was performed in accordance with institutional guidelines and was approved by the Animal Experimentation Committee of the Central Institute for Experimental Animals.

2.2. Histology and immunohistochemistry

Formalin-fixed and paraffin embedded (5 μm) sections were used for immunohistochemical staining with Cytokeratin (8/18) (h-CK8/18), HLA class I-A, B, C, asialoglycoprotein receptor 1 (ASGR1), albumin, glutamine synthetase (GS) antibodies. To estimate the replacement index (RI), which is the percentage of donor human liver cells in recipient livers, the ratio of the area occupied by h-CK8/18-positive cells to the entire area examined in immunohistochemical sections of three to five lobes was measured.

2.3. Immunoblotting

Human albumin, complement C3 protein, transferrin, and ceruloplasmin secretion was analyzed by Immunoblotting with specific primary antibodies and horseradish peroxidase-labeled secondary antibodies. The general information about the antibodies used for detection of the human protein are provided in the supplementary materials and methods.

2.4. Oligonucleotide array hybridization

Global gene expression was analyzed using the HG-U133A Plus 2 GeneChip array (Affymetrix Inc., Santa Clara, CA). Signal intensity for each transcript (background subtracted and adjusted for noise) and detection call (present, absent, or marginal) were determined using Affymetrix Expression Console Software (Affymetrix Inc.). The signal was normalized by house keeping gene, the human 18S rRNA gene (10098_M_at probe). The MIAME compliant microarray data was deposited in the Center for Information Biology gene EXpression database (CIBEX) at DDBJ (Japan) (CIBEX Accession: CBX102).

2.5. Statistical analyses

Statistical analyses were performed with the Prism 5 software (GraphPad Software, CA, USA) and SAS preclinical package software ver. 5.0 (SAS Institute, Tokyo, Japan).

3. Results

3.1. A reconstituted 'humanized liver' in TK-NOG mice can be stably maintained

Targeted HSVtk expression has previously been used to ablate specific cell types in transgenic mice [12–14]. Therefore, we used an albumin promoter to drive the liver-specific expression of a HSVtk transgene in severely immunodeficient NOG mice [15] to produce TK-NOG mice. Administration of GCV, a drug that is not toxic to human or mouse tissues, induces tissue-specific ablation of transgenic liver parenchymal cells. Since HSVtk catalyzes GCV phosphorylation, which is the rate-limiting step that cannot be performed in mammalian cells lacking this transgene, liver cells expressing the transgene are selectively destroyed. The HSVtk transgene construct, mouse breeding, protocol variables, and the properties of TK-NOG mice are described in the supplementary information and in Fig. S1. We developed an initial protocol that enabled transplanted human liver cells to replace mouse liver. A dose of GCV (0.5–5 mg/kg I.P) that is not toxic to human or mouse tissues was administered on days seven and five prior to transplantation, and 10^6 human liver cells were transplanted via intra-splenic injection. Despite using a non-optimized protocol in the initial pilot studies, a substantial amount of human albumin (hAlb) was detected in the plasma obtained from all 123 TK-NOG recipients after human liver cell transplantation, and the hAlb levels increased steadily to a maximal plasma concentration of 5.9 mg/mL (average 1.5 mg/mL; Table 1; Fig. S2A). The extent of human liver replacement was highly correlated with the measured hAlb levels ($r^2 = 0.9471$; Fig. S2B), and the engrafted human liver cells were incorporated into the existing liver in recipient ('humanized' TK-NOG) mice (Fig. 1A). After optimization of the variables (age of mice at time of transplantation, dose/timing of GCV administration) as described in the supplementary information and Fig. S3, the hAlb concentration (average 3.3 mg/mL) and level of human engraftment (average 43%) in TK-NOG mice was substantially increased (Table 1). It has recently been reported that transplantation of an increased number of human cells increases the level of human liver chimerism in $Fah^{-/-}$ model [4]. However, the average level of human reconstitution (43%) in TK-NOG liver is already at or above that obtained when this modification was used in the $Fah^{-/-}$ mouse. However, it is possible that increasing the number of transplanted human cells could further increase liver chimerism in TK-NOG mice.

Of importance, the 'humanized' TK-NOG livers maintained their synthetic function for a prolonged period. Humanized TK-NOG mice maintained a very high plasma hAlb level over a 8-month period of observation, and did not experience any loss of body weight (Fig. 1B). The functioning human liver was maintained despite the fact these mice did not receive any medication other than the GCV, which was administered prior to transplantation. This prolonged period of human liver survival has not been achieved

Table 1
Engraftment of human liver cells and repopulation rates in chimeric mice using a pilot or optimized transplantation protocol.

Pilot		Optimized		
Mice (*n*)	hAlb (mg/mL)	Mice (*n*)	hAlb (mg/mL)	Chimerism (%)
39	0.2	5	0.8	13.4
26	0.7	14	1.6	22.5
29	1.5	8	3.3	41.9
18	3.2	10	4.5	55.7
8	4.7	1	6.9	83.1
3	5.7	5	7.8	93.4
Total, 123	Average, 1.5	Total, 43	Average, 3.3***	Average, 42.5

The amount of human albumin (hAlb) in plasma and extent of human liver replacement was measured after TK-NOG mice were transplanted with human liver cells using non-optimized pilot or optimized protocols. The extent of human liver chimerism was estimated as a function of the hAlb concentration, which was shown to correlate with the extent of human liver replacement. Protocol optimization (age at time of transplantation and GCV regimen) significantly increased the extent of humanization relative to that obtained in the pilot studies.
*** Mann–Whitney test, difference of $P < 0.0001$.

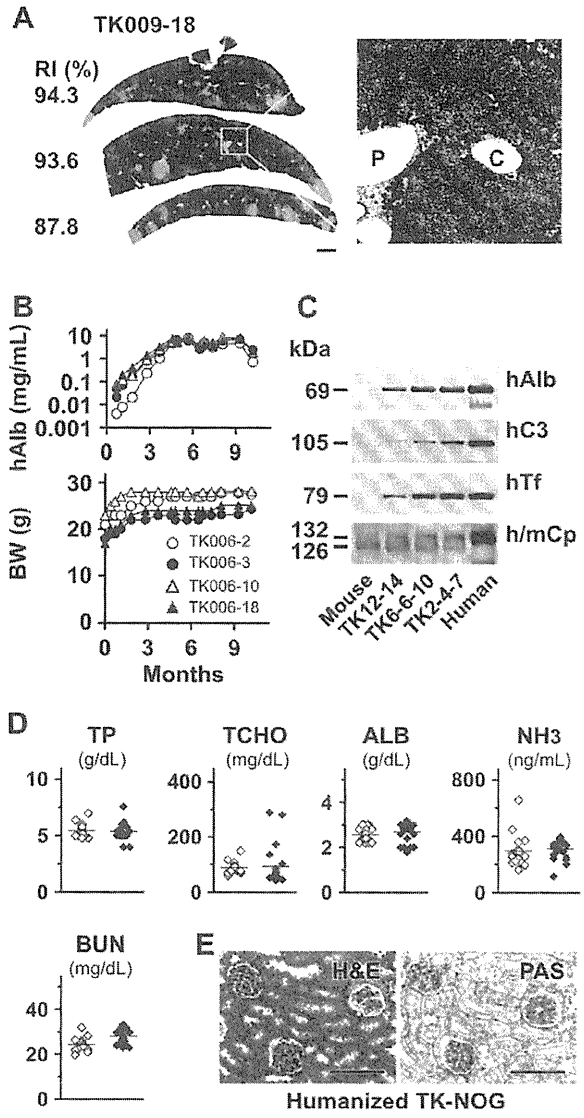

Fig. 1. (A) Reconstituted 'humanized liver' in TK-NOG mouse. Immunohistochemical staining of sections obtained from TK009-18 liver using h-CK8/18 antibody. The RI (%) for each section is indicated. Scale bar: 1 mm. An enlarged view of the boxed area is shown in the inset right. P, portal tract; C, central vein. (B) The human albumin (hAlb) level in the plasma of four TK-NOG mice and their body weight (BW) was measured over a 9-month period after GCV conditioning and human liver cell transplantation. (C) Immunoblot analyses of sera from three humanized TK-NOG mice with antibodies for specific for human albumin (hAlb), complement C3 proteins (hC3), transferrin (hTF), and for human and mouse ceruloplasmin (h/mCp). The RI of these mice (TK12-14, 6-6-10, and 2-4-7) mice were approximately 10%, 30%, and 85%, respectively. (D) Comparison of total protein (TP), total cholesterol (TCHO), albumin (ALB), ammonia (NH_3), and serum blood urea nitrogen (BUN) levels between the control NOG and humanized TK-NOG mice. The hAlb level in all of the humanized mice is >3 mg/mL. Open rhomboid, control NOG mice; filled rhomboid, humanized TK-NOG mice. (E) H&E and PAS staining of kidney obtained from a humanized TK-NOG mouse (hAlb > 5.0 mg/mL). Scale bars: 100 μm.

using uPA-dependent models. The *Fah*$^{-/-}$ model could provide a more stable humanization model; Bissig et al. achieved a long-term (34 weeks) reconstitution of *Fah*$^{-/-}$ mice as an experimental model for hepatitis C virus treatment [4]. However, long-term maintenance of these mice required repeated cycles of exposure to a drug (NTBC; 2-(2-nitro-4-trifluoro-methylbenzoyl)-1,3-cyclohexanedione) to prevent hepatocellular carcinomas, which will develop from the remaining mouse hepatocytes [4].

Serum proteins were analyzed in detail in three humanized TK-NOG mice by immunoblot analysis. Multiple different human proteins (albumin, complement C3, transferrin, and ceruloplasmin) were detected in their sera (Fig. 1C). The presence of the 105 kDa human C3 α chain in serum was of interest, since it indicates that the C3 precursor protein was processed by C3 convertase [16]. Although a high serum concentration of human C3 was thought to contribute to the renal failure that develops in uPA transgenic mice [5], humanized TK-NOG mice did not develop any biochemical or histologic evidence of kidney failure (Fig. 1D and E). Measurement of the serum total protein (TP), total cholesterol (TCHO), albumin (ALB), and ammonia (NH_3) indicated that the humanized liver had normal synthetic and metabolic function (Fig. 1D).

We further examined the histology of the humanized TK-NOG liver. In hematoxylin and eosin (H&E) stained sections, the human hepatocytes (HLA, ASGR1 and human albumin-positive) could be clearly distinguished by their size and pale cytoplasm from mouse hepatocytes (Fig. 2A), which is consistent with previous descriptions [11,17]. Periodic acid-Schiff (PAS) staining revealed that glycogen accumulation was restricted to the cytoplasm of the human hepatocytes. Most human hepatocytes (h-CK8/18-positive) were present as small foci that appeared to grow by clonal expansion within host parenchyma within 6 weeks after transplantation. There is a possibility that the reconstituted liver could be derived from a fusion between human and mouse hepatocytes [18]. However, double-immunofluorescent staining with antibodies specific for human or mouse albumin as well as PCR analysis of genomic segments within tissues isolated by laser-capture microdissection indicated that there was no evidence for fusion events between mouse and human cells (Fig. S4).

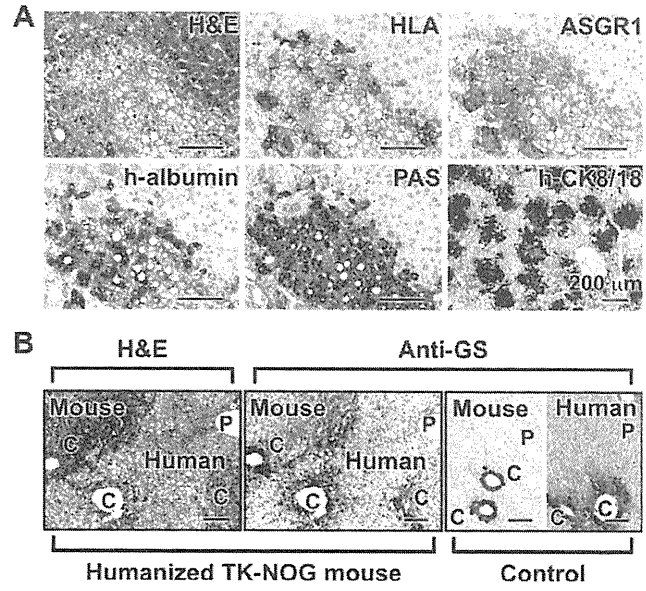

Fig. 2. (A) Histology and immunohistochemistry of the liver of humanized TK-NOG mice. Serial liver sections were stained for H&E, HLA, ASGR1, h-albumin, PAS, and h-CK8/18. Scale bars: 100 μm. (B) The position-specific pattern of GS expression within the liver lobule. H&E and immunohistochemical staining with anti-GS antibody in liver sections obtained from humanized TK-NOG mice 14 weeks after transplantation of human liver cells. The 'Mouse' and 'Human' hepatocyte boundary is indicated by a dashed line in the images on the left. Liver sections from control NOG or human liver sections that were stained with the anti-GS antibody are shown on the right. Scale bars: 100 μm. P, portal tract; C, central vein.

3.2. The gene expression profile in reconstituted TK-NOG liver resembles human liver

We also evaluated global gene expression patterns in humanized TK-NOG liver using microarrays. There was a very high level of correlation between the gene expression profiles in TK-NOG humanized liver tissue and that in the transplanted donor human liver cells ($r^2 = 0.7219$; Fig. 3A). There was only a minimal level (8%) of probes on the human gene expression array that cross-hybridized with murine mRNA (Fig. S5A). Since these mice could be used to evaluate drug metabolism, the level of expression of 26 drug metabolism-related mRNAs were also evaluated by quantitative PCR (qPCR) analyses, including: 12 CYP450 and two phase II enzymes, five SLC, and four ABC transporters, and three nuclear hormone receptors. All of the mRNAs that were expressed in donor liver cells were reproducibly expressed at comparable levels in the livers obtained from four humanized TK-NOG mice (Fig. 3B). The microarray and qPCR results were highly correlated ($r^2 = 0.9784$; Fig. S5B). In addition, there was abundant expression of human CYP3A4 in the liver of humanized TK-NOG mice (Fig. S6).

3.3. Functional analyses of the reconstituted 'humanized liver' in TK-NOG mice

We also investigated whether the reconstituted 'humanized liver' had the three-dimensional architecture characteristic of mature human liver. Since glutamine synthetase (GS) is normally expressed within a narrow zone around the central vein of the liver lobule [19], its pattern of expression in control NOG and in humanized TK-NOG livers was examined. There was no evidence for zonal GS expression within liver lobules containing human hepatocytes 6 weeks after transplantation, which suggested an immature lobular organization at this time (data not shown). In contrast, at 14 weeks after transplantation, GS had pericentral expression in the human-derived regions of the reconstituted TK-NOG liver (Fig. 2B). Thus, after 14 weeks, a mature hepatic architecture is formed in the reconstituted humanized liver in TK-NOG mice, which is in agreement with prior studies indicating that zonation occurs 8 weeks after autologous liver cell transplantation [20].

To determine whether human-specific drug metabolism could occur in the humanized TK-NOG liver, we measured the metabolism of debrisoquine (DEB), a prototypical CYP2D6 substrate that is converted to its 4-OH metabolite (4-OH DEB) by *CYP2D6*. Since mice are relatively deficient in this activity [21], an increase of 4-OH DEB production indicates that human (CYP2D6-mediated) drug metabolism is occurring in the humanized liver. A single oral dose of DEB (2.0 mg/kg) was administered to control NOG and to humanized TK-NOG mice (>4.5 mg/mL hAlb), and the amount of DEB and 4-OH DEB in serum was measured as a function of time after dosing (Fig. 3C). The area under the plasma concentration–time curve (AUC) for DEB showed no significant difference between humanized TK-NOG ($n = 6$) and NOG ($n = 9$) mice

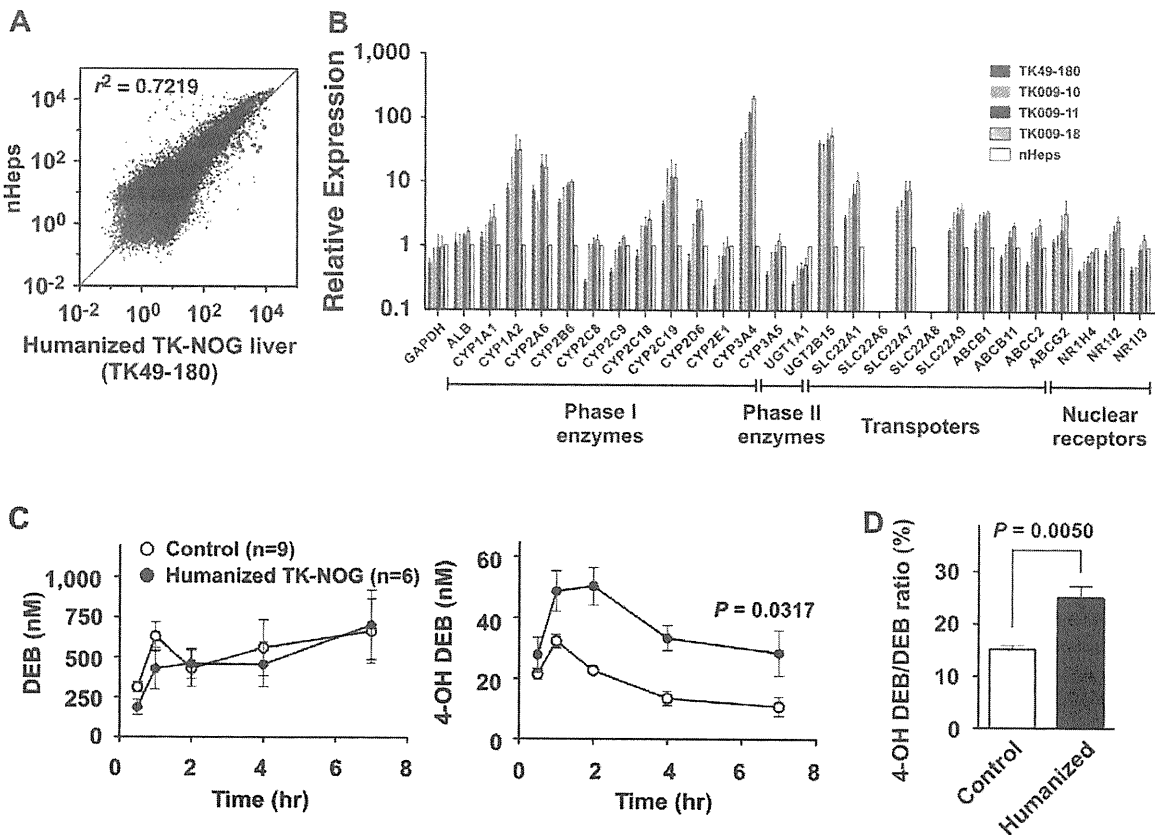

Fig. 3. (A) Gene expression within the reconstituted 'humanized liver' of TK-NOG mice. Global gene expression profiles within a fully humanized TK-NOG liver (RI of >85%) and donor human liver cells were compared by microarray analysis. The blue and black triangles indicate 'absent or marginal' and 'present' detection calls, respectively. The red circles indicate the probe sets for mRNAs related to drug metabolism. (B) The relative expression of 26 human drug metabolism related mRNAs in four independent 'humanized' TK-NOG livers and in donor human liver cells (nHeps) was assessed by qPCR. Each bar represents the average of three independent determinations and the standard error is shown. (C) Human (CYP2D6)-specific drug biotransformation in humanized TK-NOG mice. The serum concentration of DEB (left panel) and 4-OH DEB (right panel) in control NOG ($n = 9$) and humanized TK-NOG ($n = 6$) mice were measured 0, 0.5, 1, 2, 4, and 7 h after administration of a single oral dose of DEB (2 mg/kg). Each data point represents the average ± SD of 6–9 independent mice tested. (D) Urine samples were collected between 0 and 7 h after DEB administration. The % ratio of 4-OH DEB/DEB excreted into urine within 7 h was compared between control NOG ($n = 9$) and humanized TK-NOG mice ($n = 6$). By all of these measures, humanized TK-NOG mice had significantly increased amounts of 4-OH DEB in the plasma and higher 4-OH DEB excretion than control NOG mice.

(3211 ± 524.1 and 3587 ± 854.0 nM·h, respectively; $p = 0.7139$). However, humanized TK-NOG mice had significantly increased amounts of 4-OH DEB in their sera, the AUC for 4-OH DEB was 2.2-fold higher in humanized TK-NOG mice than in NOG mice (247.7 ± 26.7 and 112.9 ± 12.6 nM·h, respectively; $p = 0.0028$). Consistent with this difference, an increased amount of the 4-OH DEB metabolite was excreted into the urine of humanized TK-NOG mice (Fig. 3D). These results indicate that the humanized liver can mediate a human CYP2D6-specific drug biotransformation.

4. Discussion

The molecular, histological and functional studies demonstrate that the reconstituted 'humanized liver' in TK-NOG mice is a mature and functional "human organ". Because of these unique properties, we believe that this model could become a preferred platform for studying many aspects of human liver physiology. A unique advantage is that the TK-NOG humanized liver and its synthetic function could be stably maintained for a long period after transplantation, without the use of exogenous drugs. The TK-NOG mice did not develop systemic morbidity (liver disease, renal disease, and bleeding diathesis), nor were drug treatments required to suppress the liver tumor development. This has not previously been achieved by any of the other (uPA and *Fah*$^{-/-}$) liver reconstitution models. The longer survival and stable humanization pattern in TK-NOG mice provides a wide time-window that facilitates drug metabolism, toxicology or other longer-term studies. In fact, their prolonged survival has enabled us to 're-use' mice in different studies.

CYP3A4 is the most abundant CYP450 enzyme in human liver, and it is able to metabolize nearly 50% of all marketed drugs [22]. The metabolism of ~30% and ~10% of marketed drugs is mediated by CYP2D6 and CYP2C19, respectively [23]. We have demonstrated that reconstituted TK-NOG mice can carry out a human-specific (CYP2D6-mediated) biotransformation of a test drug. Furthermore, a large number of human phase I and II enzymes, transporters, and nuclear receptors also expressed in the humanized TK-NOG liver. The murine organs mediate many important extra-hepatic components of drug clearance (renal clearance, intestinal absorption, and metabolism, etc.) in this model system. Nevertheless, this data indicates that the humanized liver in TK-NOG mice holds great promise as a model system for studying the hepatic component of human drug metabolism. The ability to maintain these mice for prolonged time periods without requiring maintenance drugs indicates that these mice could be especially valuable for toxicological studies that require a prolonged period of drug administration.

The TK-NOG model also has another unique advantage; additional GCV doses can be administered after human cells have repopulated the liver. This enables a 'mop up' strategy to be developed to ablate residual mouse hepatic cells after human cell reconstitution, which could ensure that a very high level of human replacement is reproducibly achieved.

Acknowledgments

We thank Dr. R.D. Palmiter for providing the plasmid p2335A-1 containing the mouse albumin enhancer/promoter gene, and M. Kuronuma, S. Inoue, Y. Ando, N. Ogata, T. Mizushima, E. Hayakawa, K. Hioki, T. Sugioka, T. Ogura, T. Kamisako, and T. Etoh for outstanding technical assistance with the animal experiments. We thank C. Yagihashi and N. Omi for technical assistance with molecular analyses, and Drs. M. Kajimura, M. Ohmura, and Y. Ohnishi for helpful discussions. This work was supported by a Grant-in-Aid for Scientific Research (17300136 and 21240042) to H.S. Design of metabolome analysis in humanized NOG mice was supported by Research and Development of the Next-Generation Integrated Simulation of Living Matter, a part of the Development and Use of the Next-Generation Supercomputer Project of MEXT. M.S. is supported by JST, ERATO, Suematsu Gas Biology Project, Tokyo 160-8582, Japan. G.P. was supported by funding from a transformative RO1 award (1R01DK090992-01) from the NIDDK.

Appendix A. Supplementary data

Supplementary data associated with this article can be found, in the online version, at doi:10.1016/j.bbrc.2011.01.042.

References

[1] H. Suemizu, M. Hasegawa, K. Kawai, K. Taniguchi, M. Monnai, M. Wakui, M. Suematsu, M. Ito, G. Peltz, M. Nakamura, Establishment of a humanized model of liver using NOD/Shi-scid IL2Rg(null) mice, Biochem. Biophys. Res. Commun. 377 (2008) 248–252.
[2] M. Dandri, M.R. Burda, E. Torok, J.M. Pollok, A. Iwanska, G. Sommer, X. Rogiers, C.E. Rogler, S. Gupta, H. Will, H. Greten, J. Petersen, Repopulation of mouse liver with human hepatocytes and in vivo infection with hepatitis B virus, Hepatology 33 (2001) 981–988.
[3] D.F. Mercer, D.E. Schiller, J.F. Elliott, D.N. Douglas, C. Hao, A. Rinfret, W.R. Addison, K.P. Fischer, T.A. Churchill, J.R. Lakey, D.L. Tyrrell, N.M. Kneteman, Hepatitis C virus replication in mice with chimeric human livers, Nat. Med. 7 (2001) 927–933.
[4] K.D. Bissig, S.F. Wieland, P. Tran, M. Isogawa, T.T. Le, F.V. Chisari, I.M. Verma, Human liver chimeric mice provide a model for hepatitis B and C virus infection and treatment, J. Clin. Invest. 120 (2010) 924–930.
[5] C. Tateno, Y. Yoshizane, N. Saito, M. Kataoka, R. Utoh, C. Yamasaki, A. Tachibana, Y. Soeno, K. Asahina, H. Hino, T. Asahara, T. Yokoi, T. Furukawa, K. Yoshizato, Near completely humanized liver in mice shows human-type metabolic responses to drugs, Am. J. Pathol. 165 (2004) 901–912.
[6] M. Katoh, T. Sawada, Y. Soeno, M. Nakajima, C. Tateno, K. Yoshizato, T. Yokoi, In vivo drug metabolism model for human cytochrome P450 enzyme using chimeric mice with humanized liver, J. Pharm. Sci. 96 (2007) 428–437.
[7] L. Lootens, P. Van Eenoo, P. Meuleman, G. Leroux-Roels, F.T. Delbeke, The uPA(+/+)-SCID mouse with humanized liver as a model for in vivo metabolism of 4-androstene-3, 17-dione, Drug Metab. Dispos. 37 (2009) 2367–2374.
[8] M. Zhao, S.A. Amiel, S. Ajami, J. Jiang, M. Rela, N. Heaton, G.C. Huang, Amelioration of streptozotocin-induced diabetes in mice with cells derived from human marrow stromal cells, PLoS One 3 (2008) e2666.
[9] O.J. Pozo, P. Van Eenoo, K. Deventer, L. Lootens, S. Grimalt, J.V. Sancho, F. Hernandez, P. Meuleman, G. Leroux-Roels, F.T. Delbeke, Detection and structural investigation of metabolites of stanozolol in human urine by liquid chromatography tandem mass spectrometry, Steroids 74 (2009) 837–852.
[10] H. Kamimura, N. Nakada, K. Suzuki, A. Mera, K. Souda, Y. Murakami, K. Tanaka, T. Iwatsubo, A. Kawamura, T. Usui, Assessment of chimeric mice with humanized liver as a tool for predicting circulating human metabolites, Drug Metab. Pharmacokinet. 25 (2010) 223–235.
[11] H. Azuma, N. Paulk, A. Ranade, C. Dorrell, M. Al-Dhalimy, E. Ellis, S. Strom, M.A. Kay, M. Finegold, M. Grompe, Robust expansion of human hepatocytes in Fah-/-/Rag2-/-/Il2rg-/- mice, Nat. Biotechnol. 25 (2007) 903–910.
[12] R.A. Heyman, E. Borrelli, J. Lesley, D. Anderson, D.D. Richman, S.M. Baird, R. Hyman, R.M. Evans, Thymidine kinase obliteration: creation of transgenic mice with controlled immune deficiency, Proc. Natl. Acad. Sci. USA 86 (1989) 2698–2702.
[13] E. Borrelli, R. Heyman, C. Arias, P. Sawchenko, R. Evans, Transgenic mice with inducible dwarfism, Nature 339 (1989) 538–541.
[14] Y. Zhang, S.Z. Huang, S. Wang, Y.T. Zeng, Development of an HSV-tk transgenic mouse model for study of liver damage, FEBS J. 272 (2005) 2207–2215.
[15] M. Ito, H. Hiramatsu, K. Kobayashi, K. Suzue, M. Kawahata, K. Hioki, Y. Ueyama, Y. Koyanagi, K. Sugamura, K. Tsuji, T. Heike, T. Nakahata, NOD/SCID/gamma(c)(null) mouse: an excellent recipient mouse model for engraftment of human cells, Blood 100 (2002) 3175–3182.
[16] V.A. Bokisch, M.P. Dierich, H.J. Muller-Eberhard, Third component of complement (C3): structural properties in relation to functions, Proc. Natl. Acad. Sci. USA 72 (1975) 1989–1993.
[17] P. Meuleman, L. Libbrecht, R. De Vos, B. De Hemptinne, K. Gevaert, J. Vandekerckhove, T. Roskams, G. Leroux-Roels, Morphological and biochemical characterization of a human liver in a uPA-SCID mouse chimera, Hepatology 41 (2005) 847–856.
[18] H. Fujino, H. Hiramatsu, A. Tsuchiya, A. Niwa, H. Noma, M. Shiota, K. Umeda, M. Yoshimoto, M. Ito, T. Heike, T. Nakahata, Human cord blood CD34+ cells develop into hepatocytes in the livers of NOD/SCID/gamma(c)null mice through cell fusion, FASEB J. 21 (2007) 3499–3510.
[19] R. Gebhardt, D. Mecke, Heterogeneous distribution of glutamine synthetase among rat liver parenchymal cells in situ and in primary culture, EMBO J. 2 (1983) 567–570.

[20] K.M. Braun, J.L. Degen, E.P. Sandgren, Hepatocyte transplantation in a model of toxin-induced liver disease: variable therapeutic effect during replacement of damaged parenchyma by donor cells, Nat. Med. 6 (2000) 320–326.
[21] Y. Masubuchi, T. Iwasa, S. Hosokawa, T. Suzuki, T. Horie, S. Imaoka, Y. Funae, S. Narimatsu, Selective deficiency of debrisoquine 4-hydroxylase activity in mouse liver microsomes, J. Pharmacol. Exp. Ther. 282 (1997) 1435–1441.
[22] S. Rendic, Summary of information on human CYP enzymes: human P450 metabolism data, Drug Metab. Rev. 34 (2002) 83–448.
[23] R. Zuber, E. Anzenbacherova, P. Anzenbacher, Cytochromes P450 and experimental models of drug metabolism, J. Cell Mol. Med. 6 (2002) 189–198.

Cancer Science
The official journal of the Japanese Cancer Association

T-cell receptor gene therapy targeting melanoma-associated antigen-A4 inhibits human tumor growth in non-obese diabetic/SCID/γc^{null} mice

Yoshitaka Shirakura,[1,2,7] Yukari Mizuno,[1,2,7] Linan Wang,[2] Naoko Imai,[2] Chisaki Amaike,[2] Eiichi Sato,[3] Mamoru Ito,[4] Ikuei Nukaya,[5] Junichi Mineno,[5] Kazutoh Takesako,[5] Hiroaki Ikeda[2,6] and Hiroshi Shiku[1,2,6]

Departments of [1]Cancer Vaccine, [2]Immuno-Gene Therapy, Mie University Graduate School of Medicine, Tsu; [3]Department of Pathology, Tokyo Medical University, Tokyo; [4]Central Institute for Experimental Animals, Kawasaki; [5]Center for Cell and Gene Therapy, Takara Bio Inc., Otsu, Japan

(Received June 20, 2011/Revised September 14, 2011/Accepted September 17, 2011/Accepted manuscript online September 23, 2011/Article first published online November 9, 2011)

Adoptive cell therapy with lymphocytes that have been genetically engineered to express tumor-reactive T-cell receptors (TCR) is a promising approach for cancer immunotherapy. We have been exploring the development of TCR gene therapy targeting cancer/testis antigens, including melanoma-associated antigen (MAGE) family antigens, that are ideal targets for adoptive T-cell therapy. The efficacy of TCR gene therapy targeting MAGE family antigens, however, has not yet been evaluated *in vivo*. Here, we demonstrate the *in vivo* antitumor activity in immunodeficient non-obese diabetic/SCID/γc^{null} (NOG) mice of human lymphocytes genetically engineered to express TCR specific for the MAGE-A4 antigen. Polyclonal T cells derived from human peripheral blood mononuclear cells were transduced with the $\alpha\beta$ TCR genes specific for MAGE-A4, then adoptively transferred into NOG mice inoculated with MAGE-A4 expressing human tumor cell lines. The transferred T cells maintained their effector function *in vivo*, infiltrated into tumors, and inhibited tumor growth in an antigen-specific manner. The combination of adoptive cell therapy with antigen peptide vaccination enhanced antitumor activity, with improved multifunctionality of the transferred cells. These data suggest that TCR gene therapy with MAGE-A4-specific TCR is a promising strategy to treat patients with MAGE-A4-expressing tumors; in addition, the acquisition of multifunctionality *in vivo* is an important factor to predict the quality of the T-cell response during adoptive therapy with human lymphocytes. (*Cancer Sci* 2012; 103: 17–25)

T-cell receptor (TCR) gene transfer using retroviral vectors has been shown to be an attractive strategy to redirect the antigen specificity of polyclonal T cells to create tumor- or pathogen-specific lymphocytes.[1–6] This approach is a promising method for the treatment of patients with malignancies that might overcome the limitations of current adoptive T-cell therapies that have been hampered by difficulties in the isolation and expansion of pre-existing, antigen-specific lymphocytes in patients.[7–10] For the treatment of metastatic melanoma, clinical trials using autologous lymphocytes that have been retrovirally transduced with melanoma/melanocyte antigen-specific TCR have reported objective cancer regression.[11,12] These reports suggest that adoptive cell therapy using TCR gene-modified lymphocytes is a promising approach to immunotherapy in cancer patients; such reports have encouraged the development of novel TCR gene therapy-based approaches.

On-target adverse events, however, have been reported for TCR gene therapies targeting melanocyte differentiation antigens, such as melanoma antigen recognized by T-cells (MART)-1 or gp100. Normal tissues in which melanocytic cells exist, such as the skin, eyes, and inner ears, exhibited severe histological destruction, especially when high-avidity TCR were used.[12] Gene-modified T cells targeting carcinoembryonic antigen also induced a severe transient inflammatory colitis that served as a dose-limiting toxicity for all three patients enrolled.[13] Case reports exploring the severe adverse events seen in patients receiving T cells transduced with chimeric antigen receptors bearing the variable regions of human epidermal growth factor receptor type 2 (HER2)/neu- or CD19-reactive antibodies have suggested that these adverse events might be related to the release of cytokines from transferred cells.[14,15] These observations highlight the potential risk in the usage of receptor genes that render T cells reactive to both tumor cells and a subset of normal cells.

Cancer/testis antigens are particularly attractive targets for immunotherapy, because of their unique expression profiles. While these antigens are highly expressed on adult male germ cells or placenta, they are typically completely absent from other normal adult tissues, and demonstrate aberrant expression in a variety of malignant neoplasms.[16,17] As adult male germ cells do not express MHC class I, $CD8^+$ effector cells theoretically ignore these cells.[18] *MAGE-A*, *-B*, and *-C* genes exhibit such an expression pattern, and their immunogenicity as targets for cancer immunotherapy has been well studied.[19–21] MAGE-A4 expression was reported in 56.6% of serous carcinoma of the ovary, 61.4% of melanoma, 28.4% of non-small cell lung carcinoma, 20% of hepatocellular carcinoma, 22.3% of colorectal carcinoma, 90.2% of esophageal squamous cell carcinoma, and 6.7% of esophageal adenocarcinoma.[22–28] These results suggest that TCR gene therapy targeting the MAGE family of antigens, including MAGE-A4, represents a promising treatment for malignancies that minimizes the risk of severe on-target toxicity. The feasibility of TCR gene therapy targeting MAGE family antigens *in vivo*, however, has not previously been evaluated.

In the present study, we isolated rearranged *TCR*$\alpha\beta$ genes from a human $CD8^+$ T-cell clone that recognizes a MAGE-A4-derived peptide, MAGE-$A4_{143-151}$, in the context of HLA-A*2402.[29] Polyclonal human lymphocytes that were retrovirally transduced with these TCR genes demonstrated stable transgene expression and specific cytotoxicity against MAGE-A4-expressing tumor cells *in vitro*.[30,31] These results prompted us to confirm the efficacy of the TCR gene-modified T cells *in vivo* prior to clinical evaluation.

In this study, we investigated if human lymphocytes genetically engineered to express this MAGE-A4-specific TCR could inhibit the growth of MAGE-A4-expressing tumors when adoptively transferred into immunodeficient non-obese diabetic/SCID/γc^{null} (NOG) mice. We evaluated the *in vivo* function of the transferred cells, as well as their migration to the tumor

[6]To whom correspondence should be addressed.
E-mail: shiku@clin.medic.mie-u.ac.jp; hikeda@clin.medic.mie-u.ac.jp
[7]These authors contributed equally to this work.

doi: 10.1111/j.1349-7006.2011.02111.x

site, and the resultant antitumor effect. We addressed if the combination of adoptive cell therapy and vaccination with peptide antigen could influence the antitumor activity of transferred cells.

Materials and Methods

Peripheral blood mononuclear cells. Peripheral blood mononuclear cells (PBMC) were isolated from healthy donors who provided informed consent. Peripheral blood mononuclear cells were cultured in GT-T503 media (Takara Bio, Otsu, Japan) supplemented with 1% autologous plasma, 0.2% human serum albumin (HSA; Sigma-Aldrich, St. Louis, MO, USA), 2.5 mg/mL fungizone (Bristol-Myers Squibb, New York, NY, USA), and 600 IU/mL interleukin-2. This study was approved by the ethics review committees of Mie University Graduate School of Medicine (Tsu, Japan) and Takara Bio.

Mice. Studies were conducted using 8-week-old female NOG mice (Central Institute for Experimental Animals, Kawasaki, Japan) that had been established as described previously.[32] Mice were maintained at the Animal Center of Mie University Graduate School of Medicine. All experimental protocols were approved by the Ethics Review Committee for Animal Experimentation (of Mie University Graduate School of Medicine).

Cell lines. The KE4 (MAGE-A4$^+$HLA-A*2402$^+$ human esophageal carcinoma), QG56 (MAGE-A4$^+$HLA-A*2402$^-$ human lung carcinoma), and T2-A*2402 (human T, B hybridoma transfected with *HLA-A*2402* cDNA)[29] cell lines were maintained in RPMI-1640 media (Sigma-Aldrich) supplemented with 10% FCS, penicillin (100 U/mL), and streptomycin (100 mg/mL).

Retroviral transduction. A retroviral vector encoding MAGE-A4-specific *TCRα* (*TRAV8-1*) and *TCRβ* (*TRBV7-9*) genes (MS-bPa retroviral vector) was described previously.[30] Peripheral blood mononuclear cells were stimulated with 30 ng/mL OKT-3 (Janssen Pharmaceutical, Titusville, NJ, USA) and 600 IU/mL interleukin-2 prior to transduction with MS-bPa particles. Briefly, retroviral solutions were preloaded onto RetroNectin-coated plates and centrifuged at 2000*g* for 2 h, then rinsed with PBS, according to the RetroNectin (Takara Bio)-bound virus infection method. Cells were then applied onto preloaded plates; PBMC transduced with the MS-bPa retroviral vector were designated as gene-modified cells. Control PBMC were treated similarly, except that MS-bPa was omitted from the cultures; these specimens were designated as unmodified cells.

Tumor challenge. KE4 tumor cells (2.5×10^6 in 0.2 mL PBS) were subcutaneously inoculated into the right flanks of mice. In the indicated experiments, QG56 tumor cells (2.5×10^6 in 0.2 mL PBS) were subcutaneously inoculated in a similar manner. Tumor size was determined by the product of perpendicular diameters measured with calipers. The mice were killed before the mean diameter of the tumor reached 20 mm, according to institutional guidelines. The statistical significance of the difference between groups in tumor growth was evaluated at the last time point.

Adoptive cell transfer. After two washes in saline containing 1% human serum albumin (HSA), gene-modified or unmodified cells (1×10^8) were suspended in 0.3 mL saline and intravenously injected into a lateral tail vein of the NOG mice. Prior to injection, gene-modified cells were analyzed for staining with MAGE-A4$_{143-151}$/HLA-A*2402 tetramer and antihuman CD8 mAb to calculate the proportion of tetramer$^+$CD8$^+$ T cells infused. When indicated, HLA-A*2402-positive PBMC were pulsed with 1 μM MAGE-A4$_{141-153}$ peptide and co-administered intravenously as a peptide vaccination.

***In vitro* stimulation and staining of cells.** Cells were incubated for 2 h at 37°C with irradiated (45 Gy) stimulator T2-A*2402 cells, which had been pulsed with 1 μM MAGE-A4$_{141-153}$ or HER2$_{63-71}$ (an irrelevant peptide with HLA-A*2402 binding activity) peptide, at an effector/stimulator ratio of four in the presence of 0.1 mg/mL phycoerythrin (PE)-conjugated anti-CD107a (BD Bioscience, San Diego, CA, USA). We then incubated samples for an additional 6 h in 1 mL/mL GolgiStop (BD Bioscience). The cells were then stained with FITC-conjugated anti-CD8 (BD Bioscience) mAb. After permeabilization and fixation using a Cytofix/Cytoperm kit (BD Bioscience) according to the manufacturer's instructions, the cells were stained intracellularly with allophycocyanin (APC)-conjugated anti-γ-interferon (IFN-γ) (BD Bioscience) and PE–Cy7-conjugated antitumor necrosis factor (TNF) (BD Bioscience) mAb.

Flow cytometric analysis. PE-conjugated MAGE-A4$_{143-151}$/HLA-A*2402 tetramer (provided by the Ludwig Institute for Cancer Research, New York, NY, USA) and FITC-conjugated antihuman CD4 (BD Bioscience), human CD8 (BD Bioscience), and PerCP–Cy5.5-conjugated antihuman CD3 (BD Bioscience) mAb were used to detect transduced TCR in specific cell populations. Polychromatic analyses were performed as previously described.[33] Cell staining data were acquired using a FACS CantoI flow cytometer (Becton Dickinson, Franklin Lakes, NJ, USA), and analyzed using FACSDiva (Becton Dickinson) and FlowJ (Tree Star, Ashland, OR, USA) software.

Immunohistochemical analysis. Formalin-fixed and paraffin-embedded specimens were used. After deparaffinization, tissue sections were pretreated with antigen retrieval solution (DAKO high pH solution, DAKO, Glostrum, Denmark) at 95°C for 20 min. As a primary antibody, antihuman CD8 (clone C8/144B; DAKO) was used. Dextran polymer method with EnVision plus (DAKO) was adopted for secondary detection. 3,3′-Diaminobenzidine was used as chromogen, and hematoxylin counterstain was performed. Infiltrated CD8-positive tumor infiltrating lymphocytes (TIL) were counted in the selected 10 independent areas with most abundant TIL infiltration. Tumor-infiltrated, CD8-positive cells per high power field (0.0625 mm^2) were counted using an ocular grid at ×400 magnification. Three independent counts were performed by a board-certified pathologist (E.S) with no knowledge of the earlier results. The average TIL counts of 10 fields was used for the statistical analyses.

Statistical analyses. Data were expressed as mean ± SD. Differences between groups were examined for statistical significance using the Student's *t*-test. A *P*-value less than 0.01 denoted a statistically-significant difference.

Results

Adoptive transfer of MAGE-A4-specific, TCR-transduced lymphocytes inhibits tumor progression in a dose-dependent and antigen-specific manner. We previously reported the successful retroviral transduction of *TCRαβ* genes recognizing the MAGE-A4$_{143-151}$ peptide in an HLA-A*2402-restricted manner into polyclonally-activated human CD8$^+$ T cells. The TCRαβ-transduced CD8$^+$ T cells exhibited IFN-γ production and cytotoxic activity against both peptide-loaded T2-A*2402 cells and human tumor cell lines, such as KE4, that express both MAGE-A4 and HLA-A*2402.[30] To confirm the efficacy of these gene-modified T cells *in vivo* prior to clinical evaluation, we examined the antitumor efficacy of adoptive cell therapy with MAGE-A4-specific *TCR* gene-modified lymphocytes into NOG mice. We anticipated that a clinical trial to evaluate this therapy would involve the transduction of polyclonally-activated PBMC with *TCR* genes, followed by the transfer of these cells into patients without purification of the CD8$^+$ T-cell subset. To mimic these conditions, the NOG mice received *TCR* gene-modified lymphocytes without further purification. The *TCR* gene-modified and unmodified cells used for the transfer experiments were stained with anti-CD8 mAb and a MAGE-A4$_{143-151}$/HLA-A*2402 tetramer that specifically detected the transduced TCR (Fig. 1A). As we reported previously, this TCR bound the tetramer in a

doi: 10.1111/j.1349-7006.2011.02111.x

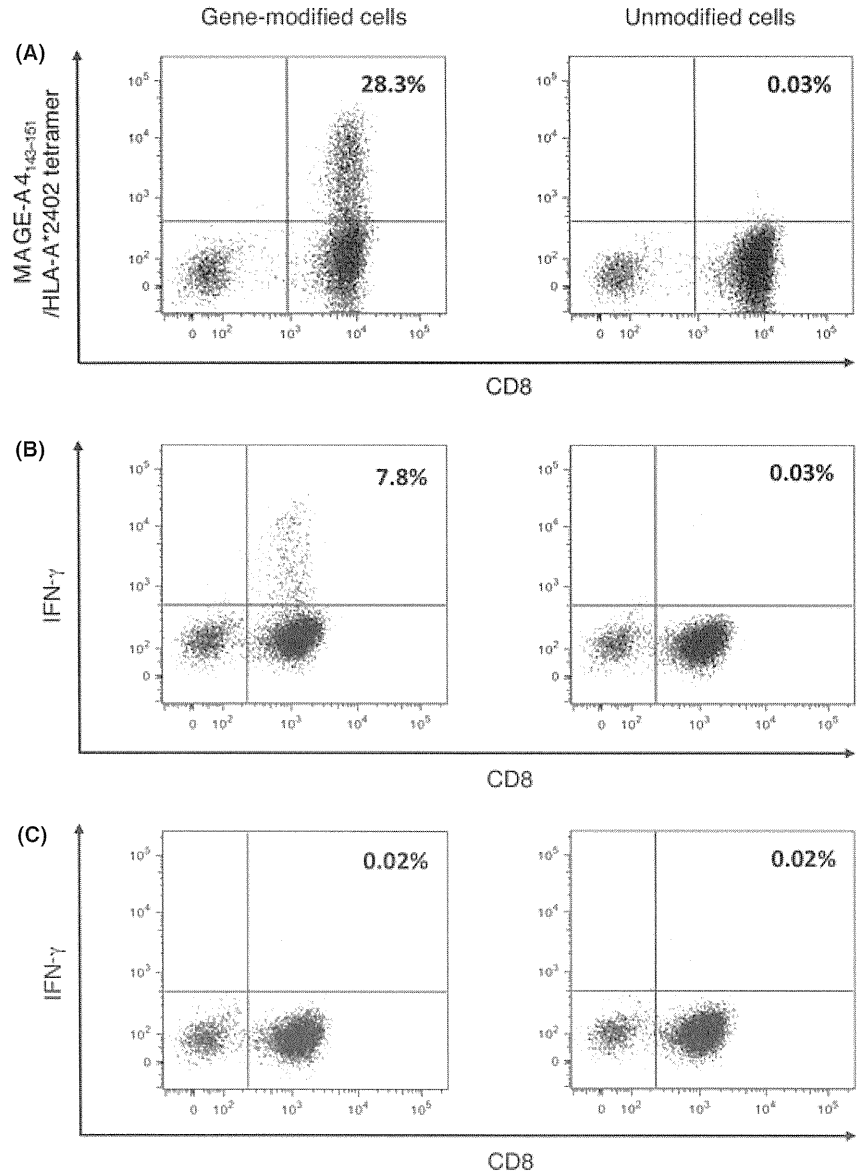

Fig. 1. Transduction of melanoma-associated antigen (MAGE)-A4-specific T-cell receptor (TCR) in human lymphocytes. Peripheral blood mononuclear cells from healthy donors were stimulated with anti-CD3 mAb and interleukin-2. Cells were cultured with or without retroviral vector encoding MAGE-A4-specific TCR, designated gene-modified or unmodified cells, respectively. (A) Representative staining for gene-modified and unmodified cells with MAGE-$A4_{143-151}$/HLA-A*2402 tetramer and antihuman CD8 mAb are shown. (B,C) Gene-modified and unmodified cells were stimulated with T2-A*2402 cells pulsed with the MAGE-$A4_{143-151}$ peptide (B) or HLA-A*2402-binding irrelevant control peptide (C). Representative specific intracellular interferon (IFN)-γ staining is displayed. Numerical value indicates the percentage of the tetramer$^+$ cells or IFN-g$^+$ cells among CD8$^+$ cells.

CD8 molecule-dependent manner.[34] These T cells were tested for specific reactivity against antigen peptide presented on HLA-A*2402 (Fig. 1B,C).

Before transfer, we stained the cells with the MAGE-$A4_{143-151}$/HLA-A*2402 tetramer to calculate the number of tetramer$^+$CD8$^+$ cells. The growth of implanted MAGE-A4$^+$HLA-A*2402$^+$ KE4 tumor cells was significantly inhibited when 9×10^6 of tetramer$^+$CD8$^+$ cells were intravenously injected into NOG mice on day 0 (Fig. 2A). The inhibition of KE4 growth required specific recognition of the MAGE-$A4_{141-153}$/HLA-A*2402 complex by the TCR, because unmodified cells derived from the same donor did not alter KE4 growth. In this experiment, 1×10^8 gene-modified or unmodified lymphocytes derived from the same donor were administered to mice. Although the CD4/CD8 ratio of the *in vitro* expanded lymphocytes depends on the donor, gene-modified and unmodified cells derived from the same donor demonstrated similar phenotypes, determined by the expression of cell surface markers, including CD3, CD4, CD8, CD45RA, CD45RO, CD62L, CCR7, CD152, CD25, CD27, and CD28 (data not shown). The growth of the QG56 tumors, which expressed MAGE-A4, but lacked HLA-A*2402, was indistinguishable in mice receiving either gene-modified or unmodified cells (Fig. 2D). Only a modest inhibition of KE4 growth was seen when mice received only 3×10^6 of tetramer$^+$CD8$^+$ cells (Fig. 2B), while no effect was seen upon administration of 1×10^6 of tetramer$^+$CD8$^+$ cells (Fig. 2C).

We addressed the effect of the adoptive transfer of the gene-modified cells into the mice with established tumors. We adoptively transferred TCR-engineered T cells into NOG mice that were inoculated with KE4 tumor cells 3 days earlier. On the day of adoptive T-cell transfer, we observed the establishment of a KE4 tumor mass in the mice. As shown in Figure 2(E), the administration of gene-modified cells significantly inhibited the growth of KE4 tumors, although the effect was limited and appeared later compared to the treatment on day 0. Taken together, the adoptive transfer of MAGE-A4-specific TCR gene-modified lymphocytes inhibited human tumor growth in NOG mice in a dose-dependent and TCR-specific manner.

Adoptively-transferred human lymphocytes persist in NOG mice. We monitored the persistence of transferred human lymphocytes in peripheral blood by staining Ficoll-purified PBMC from NOG mice with mAb specific for human CD8 and CD4.

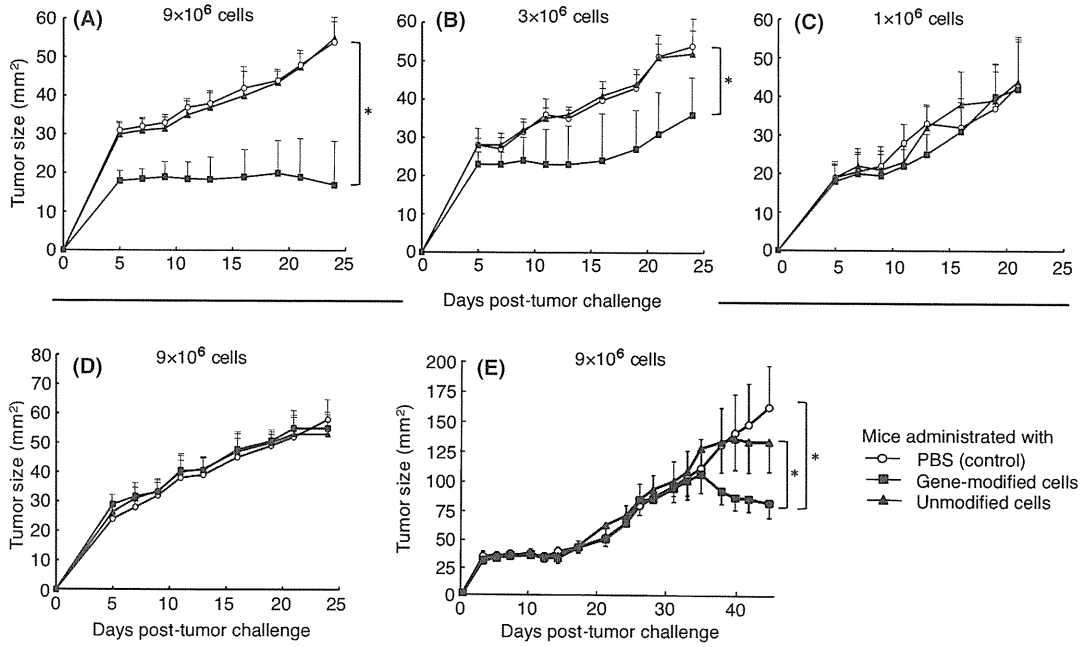

Fig. 2. Adoptive transfer of lymphocytes genetically engineered to express MAGE-A4-specific T-cell receptor inhibits human tumor progression in non-obese diabetic/SCID/γc^{null} mice. Non-obese diabetic/SCID/γc^{null} mice (n = 4 per group) were subcutaneously inoculated with 2.5×10^6 KE4 (A–C) or QG56 (D) tumor cells, and intravenously administered ~1×10^8 gene-modified (■) or unmodified (▲) cells or PBS alone (control, ○) on day 0. Total of 9×10^6 (A,D), 3×10^6 (B), or 1×10^6 (C) tetramer$^+$CD8$^+$ cells were confirmed to be adoptively transferred; we subsequently monitored tumor growth over time. (E) Non-obese, diabetic/SCID/γc^{null} mice (n = 4 per group) received the treatment 3 days after the subcutaneous inoculation of 2.5×10^6 KE4. Total of 9×10^6 tetramer$^+$CD8$^+$ cells were transferred. Mean tumor size for each group is represented as the average + SD of four mice. Results are representative of three independent experiments. Differences between groups were examined for statistical significance using the Student's t-test. *$P < 0.01$. Numerical value indicates the number of tetramer$^+$CD8$^+$ cells administrated.

Human CD8$^+$ T cells persisted in NOG mice for more than 40 days after transfer (Fig. 3A). The transferred human CD8$^+$ cells comprised between 10% and 30% of the total peripheral mononuclear cells in NOG mice at almost all time points following transfer of 1×10^8 human lymphocytes. In these experiments, approximately 9×10^6 of the transferred 1×10^8 gene-modified cells were tetramer$^+$CD8$^+$. The percentage of specifically staining cells in the total peripheral mononuclear cell population was significantly less when mice received 5×10^7 human lymphocytes (Fig. 3B). There was no significant difference in transferred cell survival or percentages between mice receiving gene-modified and unmodified cells (Fig. 3A,B). Human CD4$^+$ cells comprised less than 10% of all lymphocytes for the first 2 weeks following transfer, but a rapid increase in this population was evident after day 21(Fig. 3C,D). This observation was consistent with reports suggesting that CD4$^+$ T cells play a dominant role in the induction of graft-versus-host (GVH) reactions in hosts receiving transfusions.[35,36] The NOG mice receiving human lymphocyte transfers demonstrated significant weight loss after day 21, a sign of GVH reactions (Fig. 3E).

Transferred TCR gene-modified T cells retain their ability to recognize specific antigens in NOG mice. Lymphocytes harvested from the peripheral blood of NOG mice administered TCR gene-modified lymphocytes were tested for their antigen-specific reactivity by intracellular cytokine staining with anti-IFN-γ mAb after incubation with peptide-loaded T2-A*2402 cells. Antigen-specific IFN-γ secretion was detectable by peripheral blood CD8$^+$ cells isolated from mice throughout the 40-day period after adoptive transfer with either 1×10^8 (Fig. 4A) or 5×10^7 (Fig. 4B) gene-modified cells. No reactivity of these lymphocytes was seen against T2-A*2402 cells without loaded peptide (data not shown). Cells from mice that received unmodified lymphocytes did not demonstrate a specific response (Fig. 4A,B). These results indicate that transferred TCR gene-modified cells remained functional *in vivo*, recognizing the MAGE-A4$_{141-153}$ peptide in the context of HLA-A*2402. When 5×10^7 cells were transferred, these cells expanded more rapidly in the early phase compared to the group with 1×10^8 cells transferred. We speculate that the adoptive transfer of a lower number of antigen-specific T cells might induce these cells to expand more rapidly *in vivo* in the early expansion phase. At the later time points, more antigen-specific cells persisted in mice receiving 1×10^8 cells.

Intratumor infiltration of transferred human CD8$^+$ T cells. To confirm the infiltration of transferred cells into tumor tissue, we examined implanted KE4 and QG56 tumors by immunohistochemical analysis. As antibodies specifically recognizing the transferred TCR (TCRα V8-1 or TCRβ V7-9) are not available, we stained tumor specimens with a mAb against human CD8. Significant infiltration of human CD8$^+$ cells was detectable in KE4 tumors harvested from mice as early as 2 weeks after the transfer of gene-modified cells (Fig. 5A,B). CD8$^+$ cell infiltration in KE4 tumor specimens in the mice that received gene-modified cells was slightly better than in the mice that received unmodified lymphocytes. However, the difference was not statistically significant (Fig. 5A,B). A similar degree of infiltration was also observed in QG56 tumors. These data were consistent with previous reports analyzing the migration of tumor-specific T cells by two-photon laser microscopy that indicated tumor-specific T cells accumulate in both antigen-positive and -negative tumor tissues to comparable extents, but at different migratory velocities, according to tumor antigen expression.[37] The KE4 tumors in mice that did not receive human lymphocytes lacked any positive staining (Fig. 5B).

Combination of TCR gene therapy and peptide vaccine enhances antitumor efficacy. In animal models of adoptive cell therapy examining the effects against murine tumors with tumor-specific CD8$^+$ T cells, *in vivo* vaccinations using agents, such as antigen-peptide or antigen-encoding viruses,

doi: 10.1111/j.1349-7006.2011.02111.x

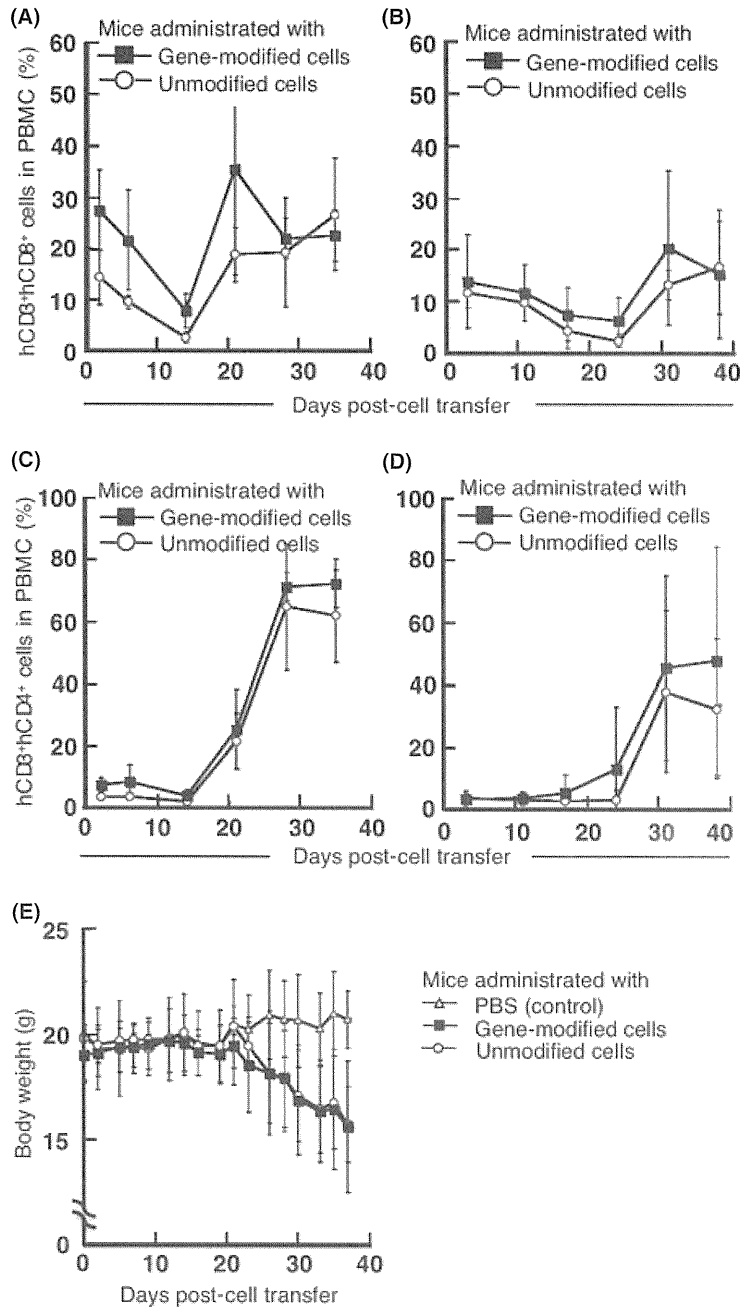

Fig. 3. Persistence of adoptively transferred human lymphocytes in non-obese, diabetic/SCID/γc^{null} (NOG) mice. Non-obese, diabetic/SCID/γc^{null} mice ($n = 4$ per group) were subcutaneously inoculated with 2.5×10^6 KE4 tumor cells, then intravenously administered 1×10^8 (A,C) or 5×10^7 (B,D) gene-modified (■) or unmodified (○) cells on day 0. Mononuclear cells were purified from peripheral blood collected from mice on the indicated days. We evaluated the proportion of human $CD3^+CD8^+$ (A,B) or $CD3^+CD4^+$ (C,D) cells among the mononuclear cell population. (E) We also monitored the body weight of NOG mice administered 1×10^8 gene-modified (■) or unmodified (○) cells or PBS (control, △) over time. Results are representative of three independent experiments. PBMC, peripheral blood mononuclear cells.

can increase the antitumor efficacy of adoptive cell therapy.[9,38] Therefore, we explored if a peptide vaccination in conjunction with TCR gene-modified cell transfer could increase the inhibition of tumor growth seen in this model. As the administration of 1×10^6 $tetramer^+CD8^+$ cells alone was incapable of inducing tumor growth inhibition in this model (Fig. 2C), we examined if the combination of an *in vivo* peptide vaccination with cell transfer under these conditions could enhance tumor inhibition. As NOG mice do not possess endogenous antigen-presenting cells capable of presenting peptide in an HLA-A*2402-restricted manner, we used HLA-A*2402-positive human PBMC pulsed with the MAGE-$A4_{143-151}$ peptide. Tumor-inoculated NOG mice receiving gene-modified cells were also administered peptide-loaded HLA-A*2402-positive PBMC derived from the same donor on days 2 and 8 of the tumor challenge. KE4 tumor growth was significantly inhibited in the mice receiving a combination of cell therapy and peptide vaccination in comparison to mice treated by cell therapy alone (Fig. 6A). The peptide vaccination did not alter KE4 growth when combined with the transfer of unmodified cells. The growth of the HLA-A*2402-negative QG56 tumor was identical in both groups (Fig. 6B).

Increased multifunctionality in adoptively-transferred cells when inoculated with peptide vaccine. We previously reported that the multifunctionality of effector cytotoxic T cells (CTL) is a critical determinant of the quality of the T-cell response and the resultant immunological control of tumor.[33,39] We therefore compared the multifunctionality of transferred cells from NOG mice treated with TCR gene-modified cells and peptide vaccination with that from mice treated by TCR gene cell therapy alone. We assessed IFN-γ and TNF-α production and CD107a mobilization by $CD8^+$ T cells at the single-cell level in specimens harvested from mice on days 2, 7, and 14 after transfer. We

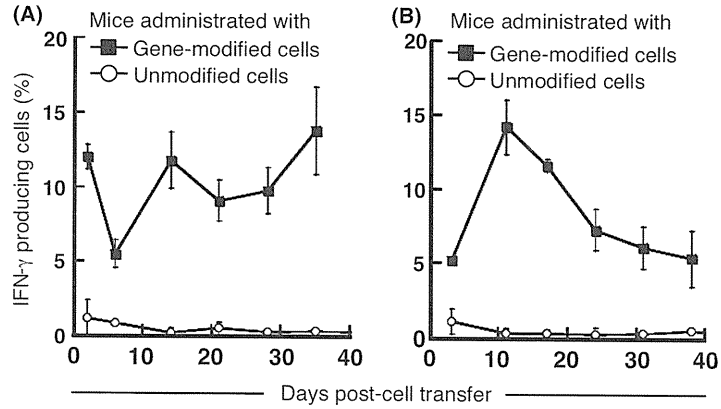

Fig. 4. Lymphocytes genetically engineered to express MAGE-A4-specific T-cell receptor-maintained specific reactivity after *in vivo* passage. Non-obese, diabetic/SCID/γc^{null} mice ($n = 4$ per group) were subcutaneously inoculated with 2.5×10^6 KE4 tumor cells, then intravenously administered 1×10^8 (A) or 5×10^7 (B) gene-modified (■) or unmodified (○) cells on day 0. Mononuclear cells were purified from peripheral blood collected from mice on the indicated days. Intracellular γ-interferon (IFN-γ) production by these cells was assessed after being stimulated with 1 μM MAGE-$A4_{141-153}$ peptide for 6 h. Data are shown as the percentage of IFN-γ-producing cells within the total human $CD8^+$ cell population. Results are representative of three independent experiments.

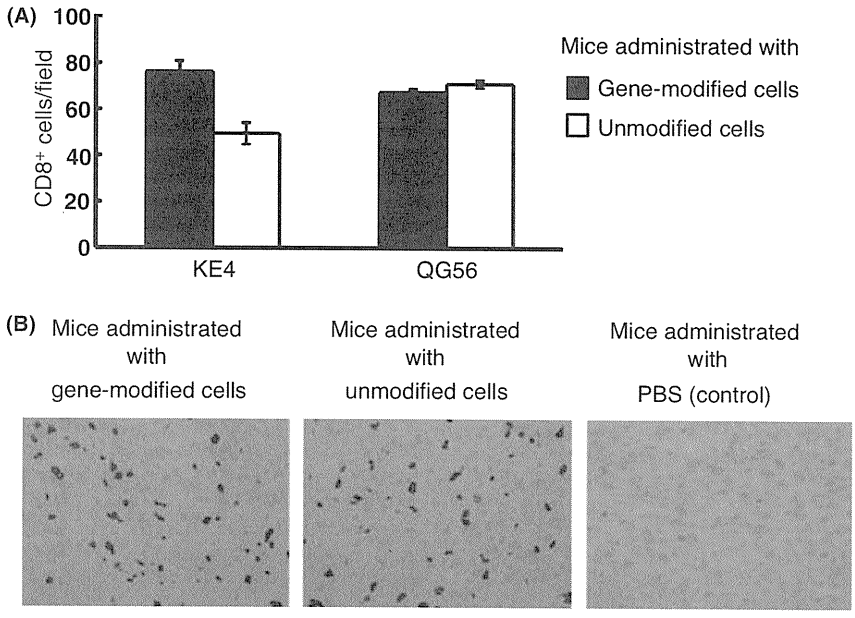

Fig. 5. Adoptively-transferred human $CD8^+$ T cells infiltrate into tumor tissues. Tumor specimens were harvested from non-obese, diabetic/SCID/γc^{null} mice 14 days after subcutaneous inoculation with 2.5×10^6 KE4 or QG56 tumor cells, and intravenous administration of 1×10^8 gene-modified or unmodified cells or PBS (control). We stained formalin-embedded tumor specimens with an antihuman CD8 monoclonal antibody, clone C8/144B. Average $CD8^+$ TIL counts ± SD in KE4 or QG56 (A) and the representative images from KE4 tissue sections (B) are shown.

selected these functional measures because multifunctionality assessed by these factors defines a sensitive correlate of the immunological control of tumors.[33,39]

The mice received human lymphocytes with or without peptide vaccination; isolated peripheral blood specimens were tested for their antigen-specific reactivity of component $CD8^+$ T cells at the indicated time points. On day 2 or 7 after adoptive transfer, we were barely able to detect cells with two or three functions in mice receiving gene-modified cells without peptide vaccination (Fig. 7); cells with three functions comprised 3.7% of all $CD8^+$ T cells, while bifunctional cells comprised 2.4% on day 14. In contrast, mice receiving combination therapy with gene-modified cells and peptide vaccination exhibited a population of cells with three and two functions of 1.4% and 2% of the total $CD8^+$ cells, respectively, as early as day 2. Therefore, multifunctional effector $CD8^+$ T cells appear earlier in mice receiving combination therapy in comparison to those receiving cell therapy alone. On day 7, trifunctional and bifunctional cells in mice receiving combination therapy comprised 1.7% and 4.8% of all cells, respectively. The cells with three or two functions were retained as part of the peripheral mononuclear cell population in these animals on day 14.

Discussion

Successful clinical responses using adoptive cell therapy with tumor-reactive T cells in patients with advanced melanoma have encouraged the development of genetic engineering approaches

doi: 10.1111/j.1349-7006.2011.02111.x

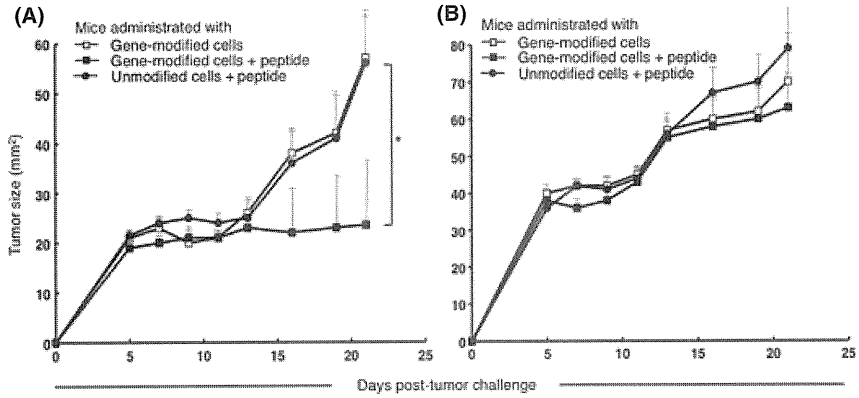

Fig. 6. Peptide vaccination enhanced the antitumor efficacy of adoptive therapy using T-cell receptor, gene-modified cells. Non-obese, diabetic/SCID/γc^{null} mice (n = 4 per group) were subcutaneously inoculated with 2.5×10^6 KE4 (A) or QG56 (B) tumor cells, and intravenously administered 1×10^8 gene-modified (□) or unmodified (●) cells on day 0. Gene-modified population included 1×10^6 tetramer$^+$CD8$^+$ cells. We pulsed 4×10^7 peripheral blood mononuclear cells derived from the same donor (HLA-A*2402 positive) with 1 μM MAGE-A4$_{141-153}$ peptide, and intravenously administered these cells into the animals on days 1 and 8 (■ and ●). Results are representative of three independent experiments.

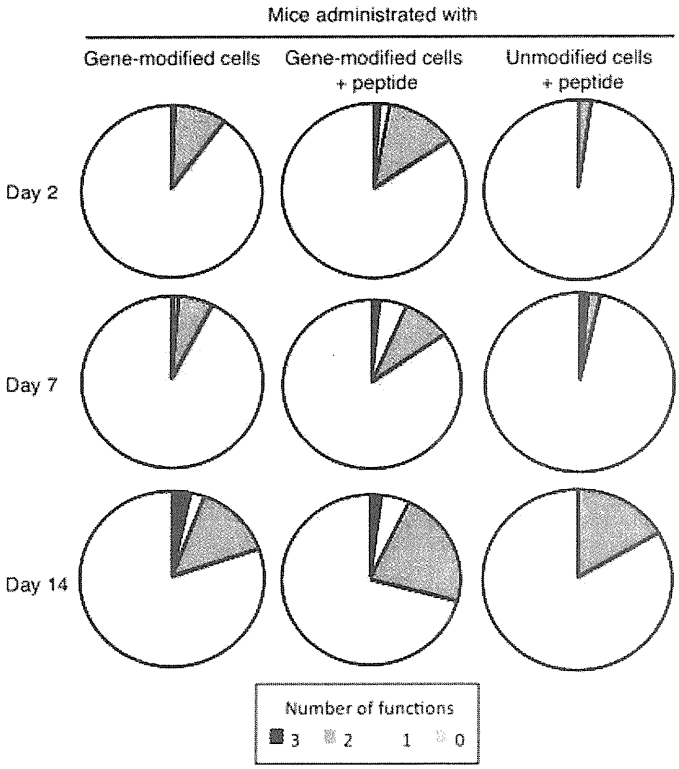

Fig. 7. Peptide vaccination increased the multifunctionality of transferred gene-modified cells. Mice were subcutaneously inoculated with 2.5×10^6 KE4 tumor cells, then intravenously administered 1×10^8 gene-modified or unmodified cells with or without peptide vaccination. Two, 7, and 14 days after transfer, we collected peripheral blood from mice. After purifying the mononuclear cells in these samples, we evaluated their multifunctionality by measuring γ-interferon (IFN-γ) and tumor necrosis factor-α (TNF-α) production and CD107a mobilization. Data are summarized in the pie chart, where each wedge represents the frequency of human CD8$^+$ cells expressing all three functions (3), any two functions (2), a single function (1), or no function (0). Results are representative of three independent experiments.

using patient lymphocytes; these studies aim to extend the range of tumor types that can be treated with this technique and to improve the quality of the lymphocytes employed.[40–42] In a recent clinical trial for metastatic synovial cell sarcoma and melanoma, patients were administered autologous lymphocytes genetically engineered to express a high-avidity TCR against NY-ESO-1; objective clinical responses were observed in four (60%) of six patients with synovial cell sarcoma, and five (45%) of 11 patients with melanoma.[43] In this trial, the transferred TCR contained two amino-acid substitutions in the third complementary determining region of the native TCRα chain that conferred CD8$^+$ T cells with an enhanced avidity. No on-target toxicities were seen in this trial, in contrast to previous observations of vigorous on-target toxicity in patients receiving lymphocytes engineered to express melanocyte differentiation antigen-specific TCR. Genetic engineering also offers the means to endow T cells with enhanced function, as well as resistance to tumor-mediated immunosuppression through the addition of genes encoding homeostatic or pro-inflammatory cytokines,[44,45] chemokine receptors,[46] anti-apoptotic molecules,[47] and costimulatory molecules,[48,49] as well as the silencing of co-inhibitory molecules,[50] although these modifications await clinical evaluation. As increased effector function and/or *in vivo* persistence of cells bearing these modifications might increase on-target toxicity during therapy, the selection of appropriate target antigens is critical to induce favorable antitumor effects and avoid severe adverse events.

The establishment of an animal model suitable for evaluating the *in vivo* efficacy and safety of human adoptive cell therapy is an important challenge to facilitate the development of these therapies and prevent toxicity. Non-obese diabetic/SCID/γc^{null}-immunodeficient mice that lack T, B, and natural killer cells, and demonstrate impaired dendritic cell activity, are a helpful animal model to evaluate the *in vivo* activity of human hematopoietic cells.[32] The NOG mouse model, however, still has limitations, including a homeostatic expansion effect on infused T cells, an allo-reactive response between infused effector cells and transplanted target cells, and potential GVH reactions. In this study, mice receiving human lymphocytes exhibited severe weight loss, consistent with GVH reaction, which worsened after day 21. Therefore, antitumor efficacy in this model is best evaluated before day 21. Future studies will need to evaluate if the homeostatic proliferation of infused cells and/or a suboptimal allo-reactivity influenced the treatment effect seen in this model. The lack of an effect by unmodified cells (Fig. 2) and the increased efficacy upon co-administration of an antigen-peptide vaccine (Fig. 6), however, strongly suggest that the observed antitumor effect was achieved in a MAGE-A4-specific, TCR-mediated manner. The future devel-

opment of improved humanized mice will help to better evaluate the optimization of human immunotherapy.

Multifunctionality is the ability of T cells to exhibit multiple functions, including the simultaneous secretion of multiple cytokines, chemokines, or cytotoxic granules at the single-cell level.[51] The importance of T-cell multifunctionality has been reported in multiple animal infection models[52,53] and in humans infected with HIV, cytomegalovirus, hepatitis B virus, or tuberculosis.[53–60] We reported the importance of effector T-cell multifunctionality in antitumor immune response. Specifically, the appearance of multifunctional $CD8^+$ effector cytotoxic T cells *in vivo* is a critical determinant of effective immunological control of tumors. Regulatory T cells were found to play a role in the inhibition of transferred tumor antigen-specific T-cell multifunctionality.[33,39] In the present study, effector T-cell multifunctionality appeared to correlate with the quality of T-cell responses in adoptive T-cell therapy utilizing genetically-engineered human lymphocytes (Figs 6,7). The peptide vaccination did not significantly change the percentage of human $CD3^+CD8^+$ cells in the PBMC of NOG mice (data not shown). The TCR-transduction efficiency in this study was not very high in general. We found that the combination of vaccination with the adoptive transfer of antigen-specific T cells increased effector T-cell multifunctionality and made the antitumor effect visible, even with a low number of specific TCR-transduced T cells transferred. The unmodified cells with background reactivity were the IFN-γ single producers. We speculate that these cells are positive for IFN-γ because of their non-specific activation due to GVH reaction.

To our knowledge, this study represents the first demonstration *in vivo* of an antitumor effect following the adoptive transfer of human lymphocytes genetically engineered to express a TCR specific for MAGE family antigen. The retroviral vector used in this report is currently under evaluation in a phase I clinical trial designed to treat patients with MAGE-A4-expressing esophageal cancer.

In summary, our data suggest that adoptive cell therapy with human lymphocytes engineered to express MAGE-A4-specific TCR through retroviral transduction is a promising strategy to treat patients with MAGE-A4-expressing tumors. Combination therapy with gene-modified cell-adoptive transfer and *in vivo* vaccination might improve antitumor efficacy, even with low numbers of transferred tumor-reactive T cells. These data support the rationale to explore clinical trials utilizing gene-modified lymphocytes prepared using the vector described in this report.

Acknowledgments

This work was supported by a Grant-in-Aid for Scientific Research from the Ministry of Education, Culture, Sports, Science and Technology of Japan.

Disclosure Statement

No potential conflicts of interest were disclosed.

References

1 Morgan RA, Dudley ME, Yu YY *et al.* High efficiency TCR gene transfer into primary human lymphocytes affords avid recognition of melanoma tumor antigen glycoprotein 100 and does not alter the recognition of autologous melanoma antigens. *J Immunol* 2003; **171**: 3287–95.
2 Rubinstein MP, Kadima AN, Salem ML *et al.* Transfer of TCR genes into mature T cells is accompanied by the maintenance of parental T cell avidity. *J Immunol* 2003; **170**: 1209–17.
3 Zhao Y, Zheng Z, Robbins PF, Khong HT, Rosenberg SA, Morgan RA. Primary human lymphocytes transduced with NY-ESO-1 antigen-specific TCR genes recognize and kill diverse human tumor cell lines. *J Immunol* 2005; **174**: 4415–23.
4 Hughes MS, Yu YY, Dudley ME *et al.* Transfer of a TCR gene derived from a patient with a marked antitumor response conveys highly active T-cell effector functions. *Hum Gene Ther* 2005; **16**: 457–72.
5 Coccoris M, Swart E, de Witte MA *et al.* Long-term functionality of TCR-transduced T cells *in vivo*. *J Immunol* 2008; **180**: 6536–43.
6 Abad JD, Wrzensinski C, Overwijk W *et al.* T-cell receptor gene therapy of established tumors in a murine melanoma model. *J Immunother* 2008; **31**: 1–6.
7 Sadelain M, Riviere I, Brentjens R. Targeting tumours with genetically enhanced T lymphocytes. *Nat Rev Cancer* 2003; **3**: 35–45.
8 Murphy A, Westwood JA, Teng MW, Moeller M, Darcy PK, Kershaw MH. Gene modification strategies to induce tumor immunity. *Immunity* 2005; **22**: 403–14.
9 June CH. Adoptive T cell therapy for cancer in the clinic. *J Clin Invest* 2007; **117**: 1466–76.
10 Rosenberg SA, Restifo NP, Yang JC, Morgan RA, Dudley ME. Adoptive cell transfer: a clinical path to effective cancer immunotherapy. *Nat Rev Cancer* 2008; **8**: 299–308.
11 Morgan RA, Dudley ME, Wunderlich JR *et al.* Cancer regression in patients after transfer of genetically engineered lymphocytes. *Science* 2006; **314**(5796): 126–9.
12 Johnson LA, Morgan RA, Dudley ME *et al.* Gene therapy with human and mouse T-cell receptors mediates cancer regression and targets normal tissues expressing cognate antigen. *Blood* 2009; **114**: 535–46.
13 Parkhurst MR, Yang JC, Langan RC *et al.* T cells targeting carcinoembryonic antigen can mediate regression of metastatic colorectal cancer but induce severe transient colitis. *Mol Ther* 2011; **19**: 620–6.
14 Morgan RA, Yang JC, Kitano M, Dudley ME, Laurencot CM, Rosenberg SA. Case report of a serious adverse event following the administration of T cells transduced with a chimeric antigen receptor recognizing ERBB2. *Mol Ther* 2010; **18**: 843–51.
15 Brentjens R, Yeh R, Bernal Y, Riviere I, Sadelain M. Treatment of chronic lymphocytic leukemia with genetically targeted autologous T cells: case report of an unforeseen adverse event in a phase I clinical trial. *Mol Ther* 2010; **18**: 666–8.
16 Boon T, Old LJ. Cancer tumor antigens. *Curr Opin Immunol* 1997; **9**: 681–3.
17 Scanlan MJ, Gure AO, Jungbluth AA, Old LJ, Chen YT. Cancer/testis antigens: an expanding family of targets for cancer immunotherapy. *Immunol Rev* 2002; **188**: 22–32.
18 Uyttenhove C, Godfraind C, Lethe B *et al.* The expression of mouse gene P1A in testis does not prevent safe induction of cytolytic T cells against a P1A-encoded tumor antigen. *Int J Cancer* 1997; **70**: 349–56.
19 van der Bruggen P, Traversari C, Chomez P *et al.* A gene encoding an antigen recognized by cytolytic T lymphocytes on a human melanoma. *Science* 1991; **254**(5038): 1643–7.
20 De Plaen E, Arden K, Traversari C *et al.* Structure, chromosomal localization, and expression of 12 genes of the MAGE family. *Immunogenetics* 1994; **40**: 360–9.
21 Chomez P, De Backer O, Bertrand M, De Plaen E, Boon T, Lucas S. An overview of the MAGE gene family with the identification of all human members of the family. *Cancer Res* 2001; **61**: 5544–51.
22 Yakirevich E, Sabo E, Lavie O, Mazareb S, Spagnoli GC, Resnick MB. Expression of the MAGE-A4 and NY-ESO-1 cancer-testis antigens in serous ovarian neoplasms. *Clin Cancer Res* 2003; **9**: 6453–60.
23 Peng JR, Chen HS, Mou DC *et al.* Expression of cancer/testis (CT) antigens in Chinese hepatocellular carcinoma and its correlation with clinical parameters. *Cancer Lett* 2005; **219**: 223–32.
24 Li M, Yuan YH, Han Y *et al.* Expression profile of cancer-testis genes in 121 human colorectal cancer tissue and adjacent normal tissue. *Clin Cancer Res* 2005; **11**: 1809–14.
25 Lin J, Lin L, Thomas DG *et al.* Melanoma-associated antigens in esophageal adenocarcinoma: identification of novel MAGE-A10 splice variants. *Clin Cancer Res* 2004; **10**: 5708–16.
26 Tajima K, Obata Y, Tamaki H *et al.* Expression of cancer/testis (CT) antigens in lung cancer. *Lung Cancer* 2003; **42**: 23–33.
27 Yoshida N, Abe H, Ohkuri T *et al.* Expression of the MAGE-A4 and NY-ESO-1 cancer-testis antigens and T cell infiltration in non-small cell lung carcinoma and their prognostic significance. *Int J Oncol* 2006; **28**: 1089–98.
28 Forghanifard MM, Gholamin M, Farshchian M *et al.* Cancer-testis gene expression profiling in esophageal squamous cell carcinoma: identification of specific tumor marker and potential targets for immunotherapy. *Cancer Biol Ther* 2011; **12**: 191–7.

doi: 10.1111/j.1349-7006.2011.02111.x

29 Miyahara Y, Naota H, Wang L *et al.* Determination of cellularly processed HLA-A2402-restricted novel CTL epitopes derived from two cancer germ line genes, MAGE-A4 and SAGE. *Clin Cancer Res* 2005; **11**: 5581–9.
30 Hiasa A, Hirayama M, Nishikawa H *et al.* Long-term phenotypic, functional and genetic stability of cancer-specific T-cell receptor (TCR) alphabeta genes transduced to CD8+ T cells. *Gene Ther* 2008; **15**: 695–9.
31 Okamoto S, Mineno J, Ikeda H *et al.* Improved expression and reactivity of transduced tumor-specific TCRs in human lymphocytes by specific silencing of endogenous TCR. *Cancer Res* 2009; **69**: 9003–11.
32 Ito M, Hiramatsu H, Kobayashi K *et al.* NOD/SCID/gamma(c)(null) mouse: an excellent recipient mouse model for engraftment of human cells. *Blood* 2002; **100**: 3175–82.
33 Imai N, Ikeda H, Tawara I, Shiku H. Tumor progression inhibits the induction of multifunctionality in adoptively transferred tumor-specific CD8+ T cells. *Eur J Immunol* 2009; **39**: 241–53.
34 Hiasa A, Nishikawa H, Hirayama M *et al.* Rapid alphabeta TCR-mediated responses in gammadelta T cells transduced with cancer-specific TCR genes. *Gene Ther* 2009; **16**: 620–8.
35 Bendle GM, Linnemann C, Hooijkaas AI *et al.* Lethal graft-versus-host disease in mouse models of T cell receptor gene therapy. *Nat Med* 2010; **16**: 565–70. 1p following 70.
36 Schroeder ML. Transfusion-associated graft-versus-host disease. *Br J Haematol* 2002; **117**: 275–87.
37 Mrass P, Takano H, Ng LG *et al.* Random migration precedes stable target cell interactions of tumor-infiltrating T cells. *J Exp Med* 2006; **203**: 2749–61.
38 Overwijk WW, Theoret MR, Finkelstein SE *et al.* Tumor regression and autoimmunity after reversal of a functionally tolerant state of self-reactive CD8+ T cells. *J Exp Med* 2003; **198**: 569–80.
39 Imai N, Ikeda H, Tawara I *et al.* Glucocorticoid-induced tumor necrosis factor receptor stimulation enhances the multifunctionality of adoptively transferred tumor antigen-specific CD8+ T cells with tumor regression. *Cancer Sci* 2009; **100**: 1317–25.
40 Dudley ME, Wunderlich JR, Robbins PF *et al.* Cancer regression and autoimmunity in patients after clonal repopulation with antitumor lymphocytes. *Science* 2002; **298**: 850–4.
41 Dudley ME, Wunderlich JR, Yang JC *et al.* Adoptive cell transfer therapy following non-myeloablative but lymphodepleting chemotherapy for the treatment of patients with refractory metastatic melanoma. *J Clin Oncol* 2005; **23**: 2346–57.
42 Dudley ME, Yang JC, Sherry R *et al.* Adoptive cell therapy for patients with metastatic melanoma: evaluation of intensive myeloablative chemoradiation preparative regimens. *J Clin Oncol* 2008; **26**: 5233–9.
43 Robbins PF, Morgan RA, Feldman SA *et al.* Tumor regression in patients with metastatic synovial cell sarcoma and melanoma using genetically engineered lymphocytes reactive with NY-ESO-1. *J Clin Oncol* 2011; **29**: 917–24.
44 Hsu C, Hughes MS, Zheng Z, Bray RB, Rosenberg SA, Morgan RA. Primary human T lymphocytes engineered with a codon-optimized IL-15 gene resist cytokine withdrawal-induced apoptosis and persist long-term in the absence of exogenous cytokine. *J Immunol* 2005; **175**: 7226–34.
45 Liu K, Rosenberg SA. Interleukin-2-independent proliferation of human melanoma-reactive T lymphocytes transduced with an exogenous IL-2 gene is stimulation dependent. *J Immunother* 2003; **26**: 190–201.
46 Kershaw MH, Wang G, Westwood JA *et al.* Redirecting migration of T cells to chemokine secreted from tumors by genetic modification with CXCR2. *Hum Gene Ther* 2002; **13**: 1971–80.
47 Charo J, Finkelstein SE, Grewal N, Restifo NP, Robbins PF, Rosenberg SA. Bcl-2 overexpression enhances tumor-specific T-cell survival. *Cancer Res* 2005; **65**: 2001–8.
48 Topp MS, Riddell SR, Akatsuka Y, Jensen MC, Blattman JN, Greenberg PD. Restoration of CD28 expression in CD28- CD8+ memory effector T cells reconstitutes antigen-induced IL-2 production. *J Exp Med* 2003; **198**: 947–55.
49 Stephan MT, Ponomarev V, Brentjens RJ *et al.* T cell-encoded CD80 and 4-1BBL induce auto- and transcostimulation, resulting in potent tumor rejection. *Nat Med* 2007; **13**: 1440–9.
50 Borkner L, Kaiser A, van de Kasteele W *et al.* RNA interference targeting programmed death receptor-1 improves immune functions of tumor-specific T cells. *Cancer Immunol Immunother* 2010; **59**: 1173–83.
51 Perfetto SP, Chattopadhyay PK, Roederer M. Seventeen-colour flow cytometry: unravelling the immune system. *Nat Rev Immunol* 2004; **4**: 648–55.
52 Chan KS, Kaur A. Flow cytometric detection of degranulation reveals phenotypic heterogeneity of degranulating CMV-specific CD8+ T lymphocytes in rhesus macaques. *J Immunol Methods* 2007; **325**: 20–34.
53 Darrah PA, Patel DT, De Luca PM *et al.* Multifunctional TH1 cells define a correlate of vaccine-mediated protection against Leishmania major. *Nat Med* 2007; **13**: 843–50.
54 De Rosa SC, Lu FX, Yu J *et al.* Vaccination in humans generates broad T cell cytokine responses. *J Immunol* 2004; **173**: 5372–80.
55 Casazza JP, Betts MR, Price DA *et al.* Acquisition of direct antiviral effector functions by CMV-specific CD4+ T lymphocytes with cellular maturation. *J Exp Med* 2006; **203**: 2865–77.
56 Betts MR, Nason MC, West SM *et al.* HIV nonprogressors preferentially maintain highly functional HIV-specific CD8+ T cells. *Blood* 2006; **107**: 4781–9.
57 Precopio ML, Betts MR, Parrino J *et al.* Immunization with vaccinia virus induces polyfunctional and phenotypically distinctive CD8(+) T cell responses. *J Exp Med* 2007; **204**: 1405–16.
58 Beveridge NE, Price DA, Casazza JP *et al.* Immunisation with BCG and recombinant MVA85A induces long-lasting, polyfunctional mycobacterium tuberculosis-specific CD4+ memory T lymphocyte populations. *Eur J Immunol* 2007; **37**: 3089–100.
59 Almeida JR, Price DA, Papagno L *et al.* Superior control of HIV-1 replication by CD8+ T cells is reflected by their avidity, polyfunctionality, and clonal turnover. *J Exp Med* 2007; **204**: 2473–85.
60 Duvall MG, Precopio ML, Ambrozak DA *et al.* Polyfunctional T cell responses are a hallmark of HIV-2 infection. *Eur J Immunol* 2008; **38**: 350–63.